Inorganic Chemistry
Cite This: Inorg. Chem. XXXX, XXX, XXX−XXX
Article
pubs.acs.org/IC

H_2MBH_2 and $M(\mu\text{-}H)_2BH_2$ Molecules Isolated in Solid Argon: Interelement M−B and M−H−B Bonds (M = Ge, Sn)

Jie Zhao,[†] Helmut Beckers,[‡] Tengfei Huang,[†] Xuefeng Wang,[*,†] and Sebastian Riedel[*,‡]

[†]School of Chemical Science and Engineering, Tongji University, Shanghai 200092, China

[‡]Institut fur Chemie und Biochemie−Anorganische Chemie, Freie Universitat Berlin, Fabeckstrase 34/36, D-14195 Berlin, Germany

Supporting Information

ABSTRACT: Laser-ablated boron atoms react with GeH_4 molecules to form novel germylidene borane H_2GeBH_2, which undergoes a photochemical rearrangement to the germanium tetrahydroborate $Ge(\mu\text{-}H)_2BH_2$ upon irradiation with light of λ = 405 nm. For comparison, the boron atom reactions with SnH_4 only gave the tin tetrahydroborate $Sn(\mu\text{-}H)_2BH_2$. Infrared matrix-isolation spectroscopy with deuterium substitution and the state-of-the-art quantum-chemical calculations are used to identify these species in solid argon. A planar structure of H_2GeBH_2 with an electron-deficient B−Ge bond with a partial multiple bond character (bond order = 1.5) is predicted by quantum-chemical calculations. In the case of $M(\mu\text{-}H)_2BH_2$ (M = Ge, Sn) two 3c−2e B−H−M hydrogen bridged bonds are formed by donation of electrons from the B−H σ-bonds into empty p-orbitals of M.

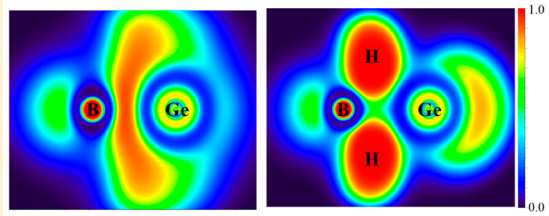

INTRODUCTION

Group 14 hydrides, such as R_3SiH, R_3GeH, and R_3SnH, are of great importance due to their industrial applications, synthetic chemistry, and the interesting nature of the chemical bonding.[1−4] Subvalent germanium and tin hydrides show a high reactivity and attracted considerable attention after the preparation of divalent tin(II)hydride $(Ar{\cdot}SnH)_2$ in 2000.[5] Several germanium(II) hydrides featuring a central GeH_2 moiety flanked by electron-donating, electron-accepting, or both groups have been prepared based on kinetic or thermodynamic stabilization.[6−9] In principle, these species representing chemical analogues to the well-known carbenes provide considerable insights into the nature of the chemical structure and bonding in subvalent group 14 compounds. Moreover, akin to transition metal hydrides, some low-valent group 14 compounds have shown to readily activate small molecules such as ammonia, dihydrogen, CO_2, ketones, as well as C═C, C−H, and C≡C bonds.[10−14] Compared to transition metal complexes the low-valent oxidation state group 14 element hydride complexes need further investigations, because of their still scarcely explored potential in many areas of synthetic chemistry and catalysis.

On the other hand, the heavier ethylene analogues like H_2EEH_2 (E = Si, Ge, Sn, Pb) are characterized by "strained" structures which show trans-bent bonding.[15−18] However, in our previous work we have shown that the H_2BSiH_2 molecule adopts a planar structure. It was prepared under cryogenic conditions in argon matrices from the reaction of laser ablated boron atoms with silane, SiH_4.[19] By this matrix-isolation technique numerous novel molecules containing BH_2 subunits have been isolated and characterized in the recent years.[20−25] In these compounds significant π-bond character has been identified based on experimental infrared and microwave spectroscopic studies. This result prompted us to investigate the reactions of laser ablated boron atoms with GeH_4 and SnH_4, and bonding characters for boron with group 14 hydrides. Here, we report experimental and computational evidence of both H_2GeBH_2 and $Ge(\mu\text{-}H)_2BH_2$ molecules isolated in cryogenic conditions in argon matrix. Interestingly, only $Sn(\mu\text{-}H)_2BH_2$ was observed in the boron atom reaction with SnH_4.

EXPERIMENTAL AND COMPUTATIONAL METHODS

Matrix-isolation experiments based on laser-ablated boron atoms in the presence of small reactant molecules seeded in a large excess of a noble gas have been described earlier.[19] The 1064 nm fundamental of a Nd:YAG laser (continuum, Minilite II; 10 Hz repetition rate) was focused on a rotating boron target. Laser-ablated enriched ^{10}B (Eagle Pitcher, 93.8% ^{10}B, 6.2% ^{11}B), and enriched ^{11}B (Eagle Pitcher, 97.5% ^{11}B, 2.5% ^{10}B), or natural boron ^{n}B (Aldrich, 80.4% ^{11}B, 19.6% ^{10}B) atoms have been codeposited with GeH_4 or SnH_4 (typically 0.3−0.5%) under excess of argon onto a 5 K CsI window. This window was mounted onto the cold tip of a closed-cycle helium refrigerator (Sumitomo Heavy Industrious, Model RDK408D). The sample preparation by laser ablation was done for 1 h at a rate of 2−4 mmol/h of the GeH_4/Ar or SnH_4/Ar mixture. After deposition, IR spectra have been recorded in the middle infrared region from 4000 to 450 cm^{-1} on a Bruker Vertex 80 V spectrometer at a resolution of 0.5 cm^{-1} using a liquid nitrogen cooled broad band MCT detector. Afterward, the matrices were annealed to allow further product formation. In the annealing process, the heat system was turned off immediately after reaching the desired temperature. Selected matrices

Received: December 11, 2017

DOI: 10.1021/acs.inorgchem.7b03109
Inorg. Chem. XXXX, XXX, XXX−XXX

were also subjected to λ = 455 and 405 nm photolysis using LED light (half-wave width 5 nm, 5 W). The GeH_4 and GeD_4 samples have been prepared by treating GeO_2 with $NaBH_4$ using Schlenk techniques.[26] A solution of $NaBH_4$ in H_2O (1 M) or $NaBD_4$ in D_2O (1 M) was slowly added to the GeO_2 slurry. The germane product was passed through a trap cooled to −120 °C and collected in two traps held at liquid nitrogen temperature at −196 °C. No further purification has been applied. SnH_4 and SnD_4 were prepared from $SnCl_2$ and $NaBD_4$ in the same method.[26]

All structures have been fully optimized at the DFT level of theory using the B3LYP[27,28] functional in conjunction with the def2-TZVPP basis sets.[29] For tin, quasi-relativistic effective core potential (ECP-28) of the Stuttgart type was used to describe 28 inner electrons.[30] Subsequent optimizations at the CCSD(T) level were carried out for the ground states of the $BGeH_4$ and $BSnH_4$ isomers. Harmonic and anharmonic frequency calculations were performed for all optimized structures. The DFT calculations were performed using GAUSSIAN 09[31] while the CCSD(T) calculations have been performed using the CFOUR program package.[32] The Multiwfn code was applied for an atoms-in-molecule (AIM) analysis and for the evaluation of the electron localization function (ELF).[33−35]

RESULTS

A series of matrix-isolation experiments have been undertaken using different GeH_4 (GeD_4) or SnH_4 (SnD_4) concentrations ranging from 0.2% to 1.0% in argon together with laser-ablated boron atoms. To control the boron atom concentration different laser energies have been applied (typically 20−30 mJ/pulse).

B + GeH_4. IR spectra of codeposited ^{10}B-enriched atoms using a 0.3% GeH_4/Ar mixture are shown in Figure 1. Two sets

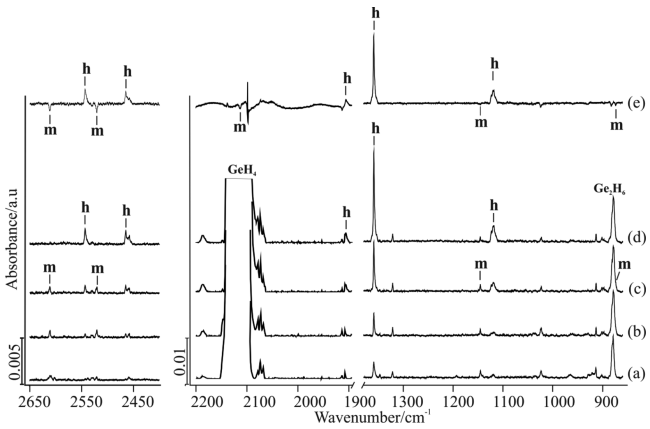

Figure 1. Infrared spectra obtained from the reaction of laser-ablated enriched boron ^{10}B atoms with GeH_4 in excess argon: (a) ^{10}B + 0.3% GeH_4 in argon codeposited for 1 h, (b) after annealing to 25 K, (c) after λ = 455 nm LED photolysis, (d) after λ = 405 nm LED photolysis, and (e) difference spectrum between traces d and c.

of absorptions have been identified based on their growth and/or decay characteristics. The first set of absorptions at 2611.4, 2520.2, 2112.7, 1145.4, and 873.6 cm^{-1} (labeled m) appeared during the sample deposition at 5 K, and increased by about 20% with subsequent annealing up to 25 K. Upon λ = 405 nm LED photolysis, this set of bands (m) nearly disappeared along with increasing bands at 2543.4, 2464.8, 1905.8, 1359.3, and 1120.1 cm^{-1} (labeled h). In experiments using ^{11}B enriched boron atoms and a mixture of 0.3% GeH_4 in argon the group m bands have been observed at 2597.6, 2516.9, 2112.7, 1138.6, and 873.6 cm^{-1} (Figure 2). Again these bands vanished upon λ = 405 nm LED photolysis and the corresponding group h bands appeared at 2529.0, 2459.8, 1902.2, 1357.9, and 1113.8 cm^{-1}.

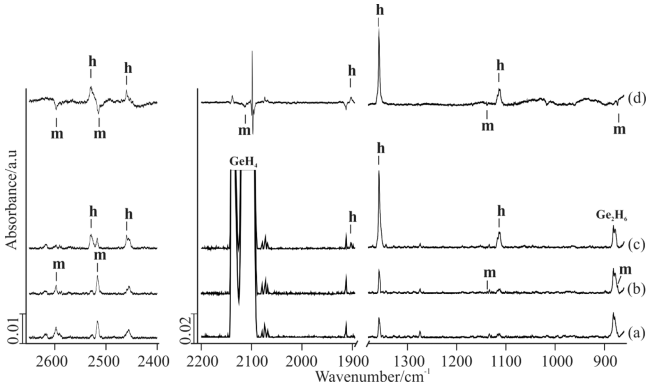

Figure 2. Infrared spectra obtained from the reaction of laser-ablated enriched boron ^{11}B atoms with GeH_4 in excess argon: (a) ^{11}B + 0.3% GeH_4 in argon codeposited for 1 h, (b) after annealing to 25 K, (c) after λ = 405 nm LED photolysis, and (d) difference spectrum between traces c and b.

Experiments using boron in natural abundance (19.8% ^{10}B, 80.2% ^{11}B) have been performed as well. Selected regions of the corresponding spectra are shown in Figure 3. Several modes of group m and group h clearly reveal the expected $^{10/11}B$ isotopic splitting and the relative intensities between the high- and low-frequency absorptions for each pair match the natural abundance of boron. Figure 4 illustrates difference spectra obtained for a 0.3% GeD_4/Ar mixture and boron atoms after λ = 405 nm LED irradiation and subsequent annealing of the matrix to 25 K, as well as a comparison of the spectra obtained from experiments using ^{10}B-enriched and natural abundant boron atoms.

In addition absorptions at 878.7 and 748.7 cm^{-1} assigned to Ge_2H_6 appeared as strong absorptions in our experiment.[36] Also other weak absorptions are observed in all laser-ablation experiments using GeH_4 due to precursor fragments and reactive species such as GeH (1813.5 cm^{-1}), GeH_2 (1839.2; 913.6 cm^{-1}), GeH_3 (2074.1; 852.4 cm^{-1}), and Ge_2H_4 (787 cm^{-1}), which have been reported previously.[36] Besides these absorptions other bands are observed owing to traces of impurities, such as H_2O, CO_2, and CO.

B + SnH_4. Figure 5 presents the IR spectra of codeposited ^{10}B enriched boron atoms using a 0.3% SnH_4/Ar mixture. One set of new absorptions at 2521.1, 2446.3, 1283.3, and 1109.4 cm^{-1} (labeled h in figures) were observed in the experiment, which appeared immediately after codeposition and slightly increased (about 20%) on the 455 nm LED irradiation. The infrared spectra in selected regions from codeposition of laser-ablated ^{11}B atoms and 0.3% SnH_4 in argon are shown in the same figure. The infrared spectra in selected regions from codeposition of laser ablated $^{10/11}B$ and 0.3% SnD_4 in argon matrix are shown in Figure 6 and all observed bands of the different isotopic substitution are summarized in Table 1.

DISCUSSION

H_2GeBH_2. As shown in Figure 1 the reaction of laser ablated ^{10}B atoms with germane leads in the formation of five bands at 2611.4, 2520.2, 2112.7, 1145.4, and 873.6 cm^{-1} (labeled m). These bands tracked together in the whole experimental process, which appeared on codeposition, increased by about

DOI: 10.1021/acs.inorgchem.7b03109
Inorg. Chem. XXXX, XXX, XXX−XXX

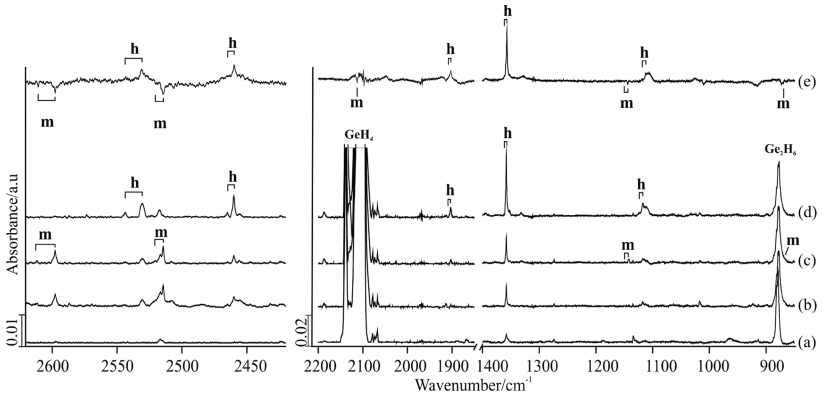

Figure 3. Infrared spectra obtained from the reaction of laser-ablated natural boron atoms with GeH_4 in excess argon: (a) ^{n}B + 0.3% GeH_4 in argon codeposited for 1 h, (b) after annealing to 25 K, (c) after λ = 455 nm LED photolysis, (d) after λ = 405 nm LED photolysis, and (e) difference spectrum between traces d and c. The $^{10/11}B$ isotope splitting of bands of the two boron compounds marked by **h** and **m** is indicated.

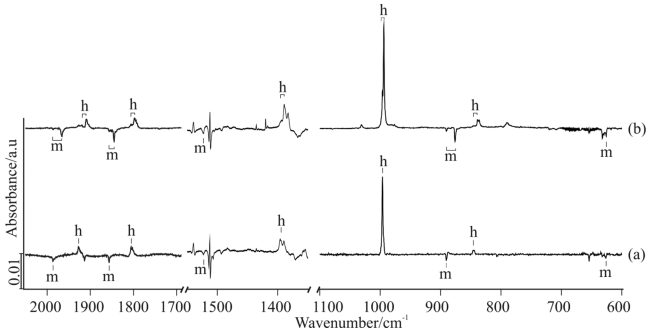

Figure 4. Difference spectrum obtained after λ = 405 nm LED photolysis of the products of the reaction between laser-ablated boron atoms and GeH_4 in excess argon and subsequent annealing to 25 K: (a) ^{10}B + 0.3% GeD_4 in argon codeposited for 1 h and (b) natural boron atoms +0.3% GeD_4 in argon codeposited for 1 h.

20% on annealing to 25 K, decreased slightly on λ = 455 nm LED photolysis, but nearly vanished upon λ = 405 nm LED photolysis. In experiments with the ^{11}B enriched isotope

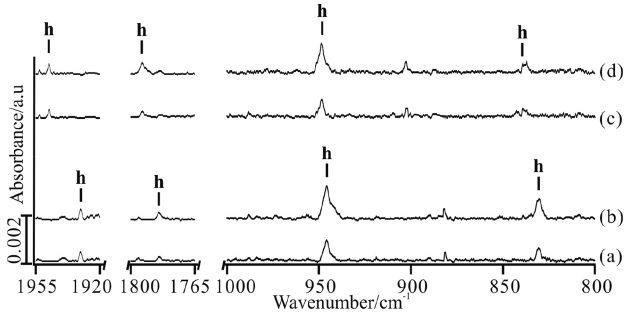

Figure 6. (a) ^{11}B + 0.3% SnD_4 in argon codeposited for 1 h, (b) after λ = 500 nm LED photolysis, (c) ^{10}B + 0.3% SnD_4 in argon codeposited for 1 h, and (d) after λ = 500 nm LED photolysis.

(Figure 2) these bands appeared at 2597.6, 2516.9, 2112.7, 1138.6, and 873.6 cm^{-1} with similar thermal and photochemical behavior, resulting in a $^{10}B/^{11}B$ isotopic ratio of 1.0053, 1.0013, 1.0000, 1.0060, and 1.0000. In the case of a target with boron in natural abundance, a series of doublet isotopic patterns at 2611.2/2597.6, 2520.7/2516.9 and 1145.4/1138.6 cm^{-1} are

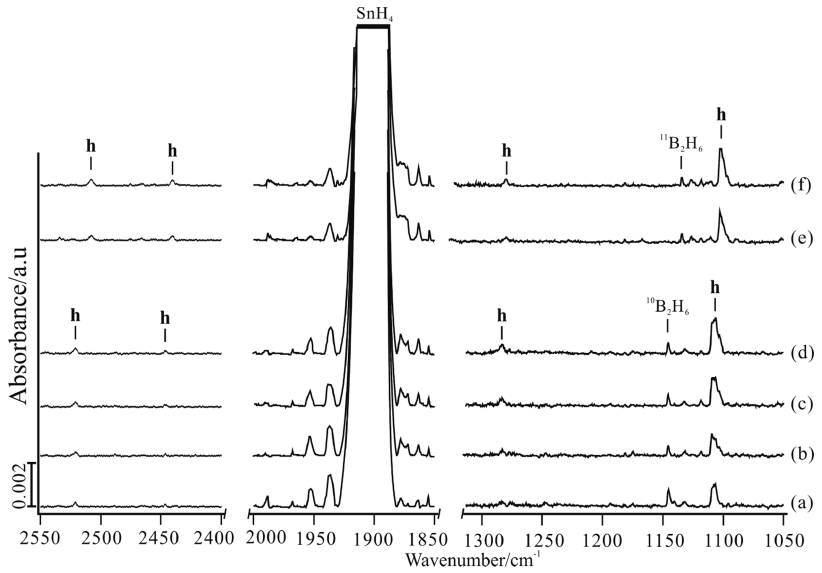

Figure 5. Infrared spectra obtained from the reaction of laser-ablated enriched boron atoms with SnH_4 in excess argon: (a) ^{10}B + 0.3% SnH_4 in argon codeposited for 1 h, (b) after annealing to 25 K, (c) after λ = 500 nm LED photolysis, (d) after λ = 455 nm LED photolysis, (e) ^{11}B + 0.3% SnH_4 in argon codeposited for 1 h, and (f) after λ = 500 nm LED photolysis.

DOI: 10.1021/acs.inorgchem.7b03109
Inorg. Chem. XXXX, XXX, XXX−XXX

Table 1. Observed Infrared Band Positions (cm^{-1}) in Solid Argon for Different Isotopologues of H_2GeBH_2, Ge(μ-H)$_2$BH$_2$, and Sn(μ-H)$_2$BH$_2$

H/^{10}B	H^{11}B	D/^{10}B	D/^{11}B	assignment
2611.4	2597.6	1986.5	1965.9	H_2GeBH_2
2520.2	2516.9	1856.4	1844.9	H_2GeBH_2
2112.7	2112.7	1523.1	1523.1	H_2GeBH_2
1145.4	1138.6	890.5	876.3	H_2GeBH_2
873.6	873.6	625.9	625.9	H_2GeBH_2
2543.4	2529	1927.5	1910.0	Ge(μ-H)$_2$BH$_2$
2464.8	2459.8	1805.5	1798.1	Ge(μ-H)$_2$BH$_2$
1905.8	1902.2	1396.2	1389.8	Ge(μ-H)$_2$BH$_2$
1359.3	1357.9	996.3	993.9	Ge(μ-H)$_2$BH$_2$
1120.1	1113.8	846.0	839.0	Ge(μ-H)$_2$BH$_2$
2521.1	2508.2	1947.6	1930.6	Sn(μ-H)$_2$BH$_2$
2446.3	2440.7	1793.5	1784.7	Sn(μ-H)$_2$BH$_2$
1283.3	1280.3	948.6	945.6	Sn(μ-H)$_2$BH$_2$
1109.4	1102.6	839.1	830.7	Sn(μ-H)$_2$BH$_2$

produced with relative intensities of approximately 1:4 (Figure 3). This clearly indicates a carrier with only one boron atom involved. The 2597.6 and 2520.7 (^{11}B + GeH$_4$) absorptions shifted to 1965.9 and 1844.9 cm^{-1} in the ^{11}B + GeD$_4$ experiments. The corresponding H/D isotopic frequency ratios of 1.3213 and 1.3642 are typical for symmetric and antisymmetric stretching vibrations of a terminal BH$_2$ group.[19] This assignment is in agreement with the two B-D stretching modes observed in the ^{10}B + GeD$_4$ experiments at 1986.5 and 1856.4 cm^{-1}, which reveal nearly identical H/D isotopic frequency ratios. The weak absorptions at 1138.6 cm^{-1} (^{11}B + GeH$_4$) and 1145.4 cm^{-1} (^{10}B + GeH$_4$) show up in the usual terminal B−H bending vibration region. Furthermore, the isotopic rations of H/D (1.2862) and ^{10}B/^{11}B (1.0060) of these absorptions are appropriate to their assignment to H−B−H bending vibration, which is 19.4 cm^{-1} lower than the terminal B−H bending mode of the known H$_2$BSiH$_2$ molecule.[19] The 2112.7 and 873.6 cm^{-1} bands show no ^{10}B/^{11}B isotopic shift, but shifted to 1523.1 and 625.9 cm^{-1}, respectively, using GeD$_4$. The corresponding H/D isotopic ratios are 1.3871 and 1.3958, which are appropriate to Ge−H stretching and bending vibrations, respectively. Notice the 873.6 cm^{-1} band appeared as a shoulder of an absorption assigned to a GeH$_2$ bending mode of the Ge$_2$H$_6$ molecule.[36] The 2112.7 cm^{-1} band is masked by the Ge−H stretching absorption of GeH$_4$ (strong broad absorptions at 2093-2143 cm^{-1}), which can be observed clearly in the difference spectra obtained before and after λ = 405 nm LED irradiation. So this group bands are appropriate for H$_2$GeBH$_2$ molecule.

Table 2. Calculated and Observed Vibrational Frequencies (cm^{-1}) and Predicted Intensities (km/mol, in Parentheses) of H_2GeBH_2 at the CCSD(T)/def2-TZVPP and B3LYP/def2-TZVPP Levels

H/^{10}B					H/^{11}B					
B3LYP		CCSD(T)			B3LYP		CCSD(T)			
harmonic	anharmonic	harmonic	anharmonic	obsd	harmonic	anharmonic	harmonic	anharmonic	obsd	assignment
2719.1 (70)	2609.4	2732.9 (69)	2624.7	2611.4	2702.9 (71)	2594.6	2716.7 (69)	2609.9	2597.6	B−H asym str
2609.7 (84)	2521.5	2628.1 (94)	2540.6	2520.2	2604.2 (82)	2515.6	2622.3 (91)	2534.3	2516.9	B−H sym str
2129.2 (118)	2161.1	2171.4 (103)	2100.7	2112.7	2129.2 (118)	2161.3	2171.4 (104)	2100.6	2112.7	Ge−H asym str
2114.2 (59)	2159.3	2161.9 (48)	2091.5		2114.2 (59)	2159.5	2161.9 (48)	2091.5		Ge−H sym str
1160.9 (33)	1138.0	1183.2 (33)	1161.2	1145.4	1153.3 (32)	1130.5	1175.0 (31)	1153.2	1138.6	BH$_2$ scissor
880.5 (60)	874.8	886.6 (55)	893.9	873.6	880.1 (60)	874.5	886.1 (55)	893.7	873.6	GeH$_2$ scissor
819.7 (11)	805.8	844.2 (14)	832.0		810.9 (11)	797.3	835.1 (14)	823.1		BH$_2$ wag
731.1 (15)	718.0	728.2 (14)	720.6		724.4 (14)	712.1	721.5 (13)	714.0		H$_2$GeBH$_2$ def
640.2 (2)	619.0	654.8 (4)	639.8		619.6 (2)	600.4	634.1 (5)	620.3		B−Ge str
398.6 (0)	363.2	419.0 (0)	409.9		398.6 (0)	363.2	419.0 (0)	410.0		H$_2$GeBH$_2$ def
393.7 (13)	400.5	384 (12)	386.6		393.7 (13)	400.6	384.0 (12)	386.6		H$_2$GeBH$_2$ def
341.4 (2)	249.2	334.3 (1)	333.2		340.9 (2)	260	333.8 (1)	333.0		GeH$_2$ wag
D/^{10}B					D/^{11}B					
B3LYP		CCSD(T)			B3LYP		CCSD(T)			
harmonic	anharmonic	harmonic	anharmonic	obsd	harmonic	anharmonic	harmonic	anharmonic	obsd	assignment
2047.4 (33)	1984.1	2056.9 (32)	1994.5	1986.5	2025.3 (33)	1963.6	2034.8 (33)	1973.9	1965.9	B−D asym str
1892 (54)	1875.9	1907.7 (62)	1904.5	1856.4	1883.2 (52)	1860.4	1898.4 (59)	1882.2	1844.9	B−D sym str
1518.4 (62)	1533.7	1548.7 (54)	1512.5	1523.1	1518.4 (62)	1533.8	1548.7 (54)	1512.6	1523.1	Ge−D asym str
1501.9 (30)	1523.6	1535.7 (24)	1499.9		1501.9 (30)	1523.0	1535.7 (24)	1500.4		Ge−D sym str
894.1 (25)	896.9	915.4 (27)	923.0	890.5	879.7 (24)	880.3	900.1 (25)	903.0	876.3	BD$_2$ scissor
645.0 (6)	636.5	665.1 (7)	657.2	625.9	633.7 (6)	625.6	653.3 (7)	645.8	625.9	GeD$_2$ scissor
629.1 (29)	626.3	633.9 (27)	631.1		628.5 (29)	625.8	633.1 (27)	630.8		BD$_2$ wag
578.3 (0)	572.6	587.8 (0)	598.2		566.8 (0)	561.0	576.8 (1)	574.5		D$_2$BGeD$_2$ def
567.0 (11)	560.2	565.4 (10)	560.3		560.3 (11)	553.8	558.7 (10)	553.9		B−Ge str
282.0 (0)	263.5	296.4 (0)	291.4		282 (0)	262.8	296.4 (0)	291.5		D$_2$BGeD$_2$ def
280.8 (7)	284.4	273.8 (6)	277.6		280.8 (7)	283.5	273.8 (6)	265.6		D$_2$BGeD$_2$ def
249.9 (1.1493)	209.7	245.2 (1)	246.3		249.5 (1)	209.1	244.8 (1)	246.0		GeD$_2$ wag

DOI: 10.1021/acs.inorgchem.7b03109
Inorg. Chem. XXXX, XXX, XXX−XXX

Table 3. Calculated and Observed Vibrational Frequencies (cm^{-1}) and Predicted Intensities (km/mol, in Parentheses) of Ge(μ-H)$_2$BH$_2$ at the B3LYP/def2-TZVPP and CCSD(t)/def2-TZVPP levels

H/^{10}B					H/^{11}B					
B3LYP		CCSD(T)			B3LYP		CCSD(T)			
harmonic	anharmonic	harmonic	anharmonic	obsd	harmonic	anharmonic	harmonic	anharmonic	obsd	assignment
2655 (86)	2535.8	2682.3 (79)	2567.6	2543.4	2639.7 (85)	2522.6	2666.8 (79)	2553.9	2529	B−H$_t$ asym str
2560.7 (88)	2461.7	2589.5 (96)	2493.3	2464.8	2555.5 (84)	2457.0	2584.0 (92)	2488.2	2459.8	B−H$_t$ sym str
2007.5 (351)	1863.2	2017.4 (352)	1896.2	1905.8	2005.2 (349)	1860.8	2015.2 (350)	1894.1	1902.2	B−H$_b$ sym str
1877 (1)	1709.4	1904.5 (0)	1747.2		1870.6 (1)	1704.7	1897.8 (0)	1742.3		B−H$_b$ asym str
1445.7 (367)	1154.6	1512.1 (418)	1384.4	1359.3	1444.7 (366)	1150.5	1511.0 (418)	1381.1	1357.9	Ge−H$_b$ sym str
1418 (26)	1272.4	1478.3 (28)	1431.6		1414.5 (27)	1266.5	1475.0 (29)	1428.1		Ge−H$_b$ asym str
1146.2 (108)	1110.2	1169.7 (98)	1139.7	1120.1	1139.9 (115)	1103.7	1163.1 (106)	1133.5	1113.8	B(H$_t$)$_2$ bend
981.1 (0)	948.3	1018.2 (0)	938.1		981.1 (0)	948.1	1018.2 (0)	937.6		Ge(μ-H)$_2$BH$_2$ def
918.1 (1)	882.7	934.4 (2)	913.4		910.8 (1)	875.5	927.0 (2)	906.2		Ge(μ-H)$_2$BH$_2$ def
778.7 (2)	663.5	807.8 (2)	758.8		772.3 (2)	656.6	801.1 (2)	751.3		Ge(μ-H)$_2$BH$_2$ def
468.6 (48)	478.9	493.7 (51)	474.3		453.7 (44)	474.9	478.1 (46)	467.6		Ge(μ-H)$_2$BH$_2$ def
197.6 (1)	163.5	204.0 (2)	262.1		197.5 (1)	170.7	203.9 (2)	266.5		Ge(μ-H)$_2$BH$_2$ def
D/^{10}B					D/^{11}B					
B3LYP		CCSD(T)			B3LYP		CCSD(T)			
harmonic	anharmonic	harmonic	anharmonic	obsd	harmonic	anharmonic	harmonic	anharmonic	obsd	assignment
1995.7 (47)	1921.1	2016.8 (44)	1946.7	1927.5	1974.6 (46)	1903.8	1995.4 (44)	1928.1	1910.0	B−D$_t$ asym str
1855.7 (68)	1801.1	1879.1 (74)	1826.3	1805.5	1847.2 (63)	1793.8	1869.9 (69)	1818.2	1798.1	B−D$_t$ sym str
1437.8 (181)	1351.2	1444.2 (183)	1409.2	1396.2	1434.6 (180)	1382.2	1441.2 (182)	1386.4	1389.8	B−D$_b$ sym str
1382.8 (1)	1289.2	1404.2 (0)	1315.3		1372.3 (1)	1280.4	1393.3 (0)	1306.1		B−D$_b$ asym str
1034.3 (186)	903.7	1082.5 (206)	1028.1	996.3	1032.4 (187)	889.4	1080.5 (209)	1025.7	993.9	Ge−D$_b$ sym str
1029.0 (12)	983.5	1070.0 (13)	1063.2		1025.1 (12)	968.7	1066.6 (13)	1054.3		Ge−D$_b$ asym str
857.4 (19)	839.3	876.0 (16)	857.9	846.0	849.5 (24)	831.7	867.7 (20)	849.9	839.0	B(D$_t$)$_2$ bend
696.5 (0)	689.1	720.3 (0)	682.1		694.0 (0)	683.5	720.3 (0)	681.3		Ge(μ-D)$_2$BD$_2$ def
694.0 (0)	687.1	708.7 (1)	705.9		689.2 (0)	679.3	701.2 (1)	689.5		Ge(μ-D)$_2$BD$_2$ def
592.4 (2)	541.0	615.5 (2)	596.0		586.3 (2)	524.1	609.0 (2)	590.0		Ge(μ-D)$_2$BD$_2$ def
431.9 (50)	414.2	453.8 (53)	446.3		421.6 (46)	401.1	443.2 (49)	436.3		Ge(μ-D)$_2$BD$_2$ def
141.5 (1)	105.3	145.5 (1)	160.9		141.4 (1)	105.3	145.4 (1)	160.8		Ge(μ-D)$_2$BD$_2$ def

Quantum-chemical calculations support the assignment. Harmonic and anharmonic frequencies calculated at the CCSD(T)/def2-TZVPP and B3LYP/def2-TZVPP levels of theory are summarized in Table 2. The $^{10}BH_2$ antisymmetric- and symmetric-stretching as well as bending modes are predicted at 2732.9, 2628.1, and 1183.2 cm^{-1} at the CCSD(T) level and therefore overestimated the experimental bands by 4.7%, 4.3% and 3.3%, respectively. The predicted Ge−H stretching and bending modes show 2.7% and 1.5% overestimation. As expected, the anharmonic corrected frequencies match the observed group m absorptions very well to only 1% of deviation for all modes. Notice this holds also for the isotopologues of H_2GeBH_2 (Table 2). For completeness, also the B3LYP functional was used leading in very similar predictions and the agreement (Table 2).

Assignment of closed-shell species H_3GeBH_2 can be ruled out based on our theoretical frequency calculations. Similarly H_3SiBH_2 was not observed in boron atom reactions with SiH_4.[19] As shown in Table S1 the strongest Ge−H stretching and bending modes for $H_3Ge^{10}BH_2$ were predicted at 2119.1 and 812.3 cm^{-1}, respectively, at B3LYP/Def2-TZVPP level. At the same level the similar Ge−H stretching and bending modes for H_2GeBH_2 were predicted at 2129.2 and 880.5 cm^{-1} (Table 2). Notice for germanium hydrides the B3LYP frequency calculations gave 0−5% overestimations,[36] and a strong absorption should appear around 770−820 cm^{-1} if H_3GeBH_2 is produced; however, there is no any band was observed in this region.

Ge(μ-H)$_2$BH$_2$. The absorptions at 2543.4, 2464.8, 1905.8, 1359.3, and 1120.1 cm^{-1} (labeled h) with ^{10}B isotopes appeared as very weak absorptions after codeposition. The bands doubled on λ = 455 nm LED irradiation and sharply increased by λ = 405 nm LED photolysis. The ^{11}B + GeH_4 reaction (Figure 2), showed red-shifted bands at 2529.0, 2459.8, 1902.2, 1357.9, and 1113.8 cm^{-1}. If naturally abundant boron was used, five pairs of bands at 2543.4/2529.0, 2464.8/2459.8, 1905.8/1902.2, 1359.3/1357.9, 1120.1/1113.8 cm^{-1} (labeled h) appeared with relative intensities of approximately 1:4. This isotope pattern again confirms the involvement of a single boron atom in the carrier molecule. The deuterated counterparts of the 2543.4 and 2464.8 cm^{-1} bands (^{10}B + GeH_4) appeared at 1927.5 and 1805.5 cm^{-1} for ^{10}B atoms with GeD_4 and at 1910.0 and 1798.1 cm^{-1} in ^{11}B + GeD_4. These bands show typical H/D ratios for the terminal antisymmetric and symmetric BH_2 stretching vibrations. The 1120.1 cm^{-1} band in the ^{10}B + GeH_4 reaction with ^{11}B counterpart at 1113.8 shifted to 846.0 cm^{-1} in the reaction of ^{10}B + GeD_4, and to 839.0 cm^{-1} in the reaction of ^{11}B + GeD_4. The band position as well as the H/D isotopic ratio (1.3240 for ^{10}B) and $^{10}B/^{11}B$ isotopic ratio (1.0057) are appropriate to a terminal BH_2 bending mode. The absorptions at 1905.8 and 1359.3 cm^{-1} (^{10}B + GeH_4) with their corresponding deuterium counterparts at 1396.2 and 996.3 cm^{-1} (^{10}B + GeD_4) show large H/D ratios (1.3650 and 1.3643) but little $^{10}B/^{11}B$ isotopic shift (ratio = 1.0019 and 1.0010), respectively. The band positions of these two modes are located much lower than terminal B−H or Ge−H stretching modes and much higher than terminal B−H or

DOI: 10.1021/acs.inorgchem.7b03109
Inorg. Chem. XXXX, XXX, XXX−XXX

Ge−H bending modes. These modes indicate the presence of bridged hydrogen atoms and the influence of two heavy atoms on these vibrational modes. In fact this set of absorptions are typical for bidentate tetrahydroborate complexes. The symmetric and antisymmetric terminal B−H_t (H_t = terminal hydrogen atom) stretches usually appear as strong sharp, doublets at 2400−2600 cm^{-1} and the symmetric and antisymmetric B−H_b (H_b = bridged hydrogen atom) stretches coupled with ring deformation usually seen as overlapped bands near 2000 cm^{-1}. In addition, M−H_b symmetric and antisymmetric stretches couple with ring deformation at 1300−1500 cm^{-1}. One additional band at 1050−1150 cm^{-1} (BH_2 deformation) is regularly observed in such species.[37] Accordingly, this group of absorptions are assigned to the Ge(μ-H)$_2$BH$_2$ molecule.

The assignment to the Ge(μ-H)$_2$BH$_2$ molecules is confirmed by the excellent agreement between observed and calculated frequencies (Table 3) of five fundamental vibrations in three different spectral regions, that is, terminal B−H_t stretching, bridged B−H_b and Ge−H_b stretching modes coupled with ring deformation, and the B(H_t)$_2$ bending mode. As shown in Table 5, the Ge(μ-H)$_2$BH$_2$ molecule is predicted to have a $^2B_2$ ground state with C_{2v} symmetry. The calculated anharmonic frequencies at the CCSD(T)/def2-TZVPP level of theory (Table 3) are in good agreement with the experimental values, with a maximum deviation of 30 cm^{-1}. The calculated isotope shifts are also in excellent agreement with the experimental values, which give additional support for its assignment. As can be seen in Table 3, the harmonic frequencies at the B3LYP/def2-TZVPP level also agree with the experimental observations. However, the bridged B−H_b or Ge−H_b stretching modes are underestimated (maximum deviation of 200 cm^{-1}) in the anharmonic frequency calculation, suggesting B3LYP calculated anharmonic frequencies cannot describe these modes correctly, although the B3LYP calculated B−H_t stretching frequencies match the experimental values very well.

Assignment of one hydrogen bridge species HGe(μ-H)BH$_2$ must be ruled out because the calculated vibrational modes (Table S3) cannot reproduce the observed frequencies. For example, the calculated strongest B−H_t bending mode is calculated at 1062.7 cm^{-1} (B3LYP), but no such a band was found in our experiments. In addition the HGe(μ-H)BH$_2$ is not stabilized in matrix due to 8 kcal/mol higher in energy than both H_2GeBH_2 and Ge(μ-H)$_2$BH$_2$ (Figure 7).

Sn(μ-H)$_2$BH$_2$. The absorptions at 2521.1, 2446.3, 1283.3, and 1109.4 cm^{-1} (labeled h) appeared after codepostion of laser ablated ^{10}B atoms with SnH_4 (Figure 5). This group of absorptions show red-shifts to 2508.2, 2440.7, 1280.3, and 1102.6 cm^{-1} in the reaction of ^{11}B + SnH_4 in argon matrix (Figure 6), and split into four pair of absorptions at 2521.1/2508.2, 2446.3/2440.7, 1355.6/1321.8 and 1109.4/1102.6 cm^{-1} with relative intensity ratios of about 1:4 using natural abundance boron as reagent. The corresponding deuterium counterparts of these four absorptions appeared at 1947.6, 1793.5, 948.6, and 839.1 cm^{-1} in the reaction of ^{10}B + SnD_4, and at 1930.6, 1784.7, 945.6, and 830.7 cm^{-1} in the reaction of ^{11}B + SnD_4 in solid argon. Analogues to the absorptions assigned to Ge(μ-H)$_2$BH$_2$, this group of absorptions are typical for the bidentate tetrahydroborate complex,[38] and are appropriate for the Sn(μ-H)$_2$BH$_2$ molecule. Unfortunately, the strong B−H_b symmetric stretching vibration calculated at 1885.3 cm^{-1} (predicted intensity = 526 km/mol) was not observed in our experiment, which may be covered by very strong Sn−H stretching mode centered at 1893.8 cm^{-1}.

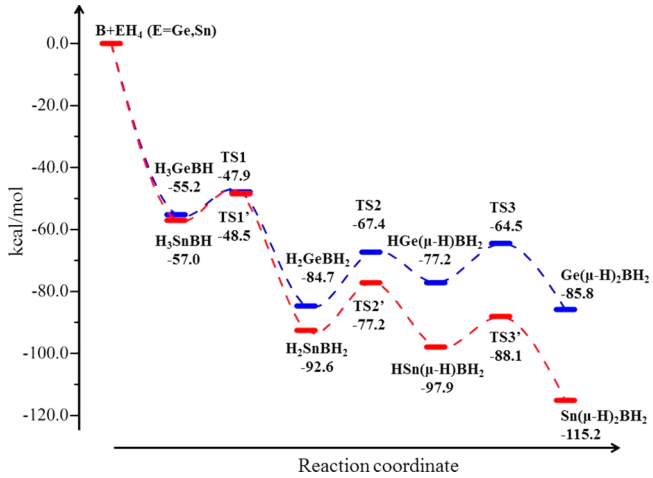

Figure 7. Potential energy surface calculated at the CCSD(T)/def2-TZVPP level of theory for the reaction of boron atoms and MH_4 (E = Ge, Sn) leading to the final product M(μ-H)$_2$BH$_2$. Transition states are calculated at the CCSD(t)//B3LYP/def2-TZVPP level.

We also failed to identify this mode by difference spectra as the yield of Sn(μ-H)$_2$BH$_2$ is much less than Ge(μ-H)$_2$BH$_2$ obtained from B + GeH_4 reaction (Figure 3). Our CCSD(t) calculations gave anharmonic frequencies (Table 4) of the terminal B−H_t antisymmetric and symmetric stretching vibration of Sn(μ-H)$_2$BH$_2$ at 2553.2 and 2478.1 cm^{-1}, the Sn−H_b symmetric stretching vibration at 1357.8 cm^{-1} and the B−H_t bending vibration at 1133.8 cm^{-1}, which match the experimental value very well (maximum deviation of 55 cm^{-1}) and support the assignment. But similar to Ge(μ-H)$_2$BH$_2$, the anharmonic frequencies calculated at B3LYP level cannot describe the Sn−H_b stretching accurately.

The calculated frequencies for closed-shell species H_3SnBH_2 are shown in Table S2, but no observed absorptions can match this molecule. In addition, we optimized HSn(μ-H)BH$_2$ and H_2SnBH_2 molecules as shown in Figure 7, which are much higher in energy than Sn(μ-H)$_2$BH$_2$ and unlikely isolated in matrix. For comparison the calculated frequencies are listed in Tables S4 and S5. The calculated much higher B−H_t stretching vibration and much lower strongest B−H_t bending vibration compared with the experimental values rule out the formation of HSn(μ-H)BH$_2$ molecule.

■ REACTION MECHANISM AND ELECTRONIC STRUCTURE

A series of work about the reaction of laser ablated boron atoms with EH_4 (E = C, Si, Ge, and Sn) were carried out to have an insight into the periodical trends of the boron bonding with group 14 hydrides.[19,39] In former matrix-isolation investigations the major products have been identified to be H_2BCH_2 in boron atom reaction with CH_4,[39] and H_2BSiH_2 and Si(μ-H)$_2$BH$_2$ with SiH_4.[19] The reaction of boron atoms with GeH_4 in argon matrix was similar to the reaction of boron with SiH_4. The H_2GeBH_2 molecules were produced in the annealing process, suggesting that the formation of H_2GeBH_2 is thermodynamically driven. Upon 405 nm LED photolysis, one electron is excited from the B−Ge π orbital to B−Ge π^* orbital (calculated at 407 nm at MCQDPT level by GAMESS-US program package),[40] leading to the cleavage of the B−Ge

DOI: 10.1021/acs.inorgchem.7b03109
Inorg. Chem. XXXX, XXX, XXX−XXX

Table 4. Calculated and Observed Vibrational Frequencies (cm^{-1}) and Predicted Intensities (km/mol, in Parentheses) of $Sn(\mu\text{-}H)_2BH_2$ at the B3LYP/def2-TZVPP and CCSD(t)/def2-TZVPP Levels

H/^{10}B					H/^{11}B					
B3LYP		CCSD(t)			B3LYP		CCSD(t)			
harmonic	anharmonic	harmonic	anharmonic	obsd	harmonic	anharmonic	harmonic	anharmonic	obsd	assignment
2634.2 (93)	2517.4	2667.3 (86)	2553.2	2521.1	2619.3 (92)	2504.3	2652 (86)	2539.6	2508.2	$B-H_t$ asym str
2543.9 (99)	2445.2	2576.6 (117)	2478.1	2446.3	2538.7 (94)	2440.7	2571 (112)	2472.6	2440.7	$B-H_t$ sym str
2016.5 (504)	1903.0	2033.8 (526)	1885.3		2013.8 (503)	1899.0	2031.2 (526)	1875.1		$B-H_b$ sym str
1928.8 (2)	1751.0	1954.6 (4)	1790.5		1922 (8)	1745.8	1947.6 (4)	1785.5		$B-H_b$ asym str
1391.0 (220)	1104.1	1451 (290)	1338.6	1283.3	1390.3 (219)	1059.4	1450.1 (290)	1334.9	1280.3	$Sn-H_b$ sym str
1318.4 (1)	1159.5	1372.4 (29)	1342.8		1313.4 (26)	1156.1	1367.6 (30)	1339.4		$Sn-H_b$ asym str
1138.5 (134)	1099.3	1166.9 (134)	1133.8	1109.4	1131.8 (143)	1092.0	1160.1 (144)	1127.3	1102.6	$B(H_t)_2$ bend
1034.3 (0)	1013.3	1070.9 (0)	1052.2		1034.3 (0)	1011.5	1070.9 (0)	1050.6		$Sn(\mu\text{-}H)_2BH_2$ def
937.6 (2)	918.1	966.9 (3)	942.5		930.2 (2)	911.1	959.3 (3)	935.4		$Sn(\mu\text{-}H)_2BH_2$ def
712.4 (5)	502.5	749.6 (5)	652.3		707.7 (4)	462.8	744.4 (4)	635.1		$Sn(\mu\text{-}H)_2BH_2$ def
426 (68)	372.3	450.4 (80)	415.8		411.8 (62)	368.8	435.5 (74)	411.0		$Sn(\mu\text{-}H)_2BH_2$ def
171.4 (0)	209.1	196.3 (0)	236.2		171.3 (0)	213.0	196.2 (0)	239.2		$Sn(\mu\text{-}H)_2BH_2$ def
D/^{10}B					D/^{11}B					
B3LYP		CCSD(t)			B3LYP		CCSD(t)			
harmonic	anharmonic	harmonic	anharmonic	obsd	harmonic	anharmonic	harmonic	anharmonic	obsd	assignment
1978.9 (49)	1908.8	2004.5 (46)	1936.7	1947.6	1958.2 (48.4)	1890.7	1983.4 (46)	1917.4	1930.6	$B-D_t$ asym str
1843.9 (77)	1788.9	1870.9 (90)	1816.9	1793.5	1835.3 (71.8)	1780.9	1861.5 (84)	1809.4	1784.7	$B-D_t$ sym str
1447.3 (250)	1397.9	1458.9 (259)	1393.9		1443.6 (250.7)	1382.6	1455.3 (261)	1378.7		$B-D_b$ sym str
1421.6 (4)	1325.7	1441.6 (2)	1350.7		1410.8 (4.3)	1313.4	1430.4 (2)	1341.4		$B-D_b$ asym str
992.3 (112)	844.5	1035.8 (144)	965.2	948.6	990.8 (112.8)	838.6	1034.1 (146)	961.6	945.6	$Sn-D_b$ sym str
968.2 (9)	912.6	1004.3 (12)	988.9		962.5 (9.9)	906.7	999.0 (12)	982.6		$Sn-D_b$ asym str
853.7 (25)	834.6	874.8 (22)	856.5	839.1	845.7 (31.6)	826.8	866.6 (29)	848.5	830.7	$B(D_t)_2$ bend
731.6 (0)	726.4	757.6 (0)	754.5		731.6 (0)	725.6	757.6 (0)	753.5		$Sn(\mu\text{-}D)_2BD_2$ def
711.1 (0)	725.9	733.2 (1)	741.3		703.6 (0.3)	709.5	725.5 (1)	726.9		$Sn(\mu\text{-}D)_2BD_2$ def
533.2 (5)	460.3	563.2 (5)	527.6		529 (4.1)	454.7	558.4 (4)	522.3		$Sn(\mu\text{-}D)_2BD_2$ def
389.1 (66)	360.6	410.7 (78)	403.6		379.3 (61.5)	352.2	400.5 (73)	393.9		$Sn(\mu\text{-}D)_2BD_2$ def
121.9 (0)	125.7	139.6 (0)	148.8		121.9 (0)	125.4	139.5 (0)	148.7		$Sn(\mu\text{-}D)_2BD_2$ def

Table 5. Structural Parameters and Electronic Structure Analysis of H_2GeBH_2, $Ge(\mu\text{-}H)_2BH_2$, and $Sn(\mu\text{-}H)_2BH_2$ Obtained at CCSD(T)/def2-TZVPP Level of Theory[a]

Structure	SOMO	ELF	AIM
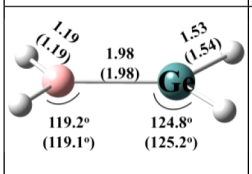	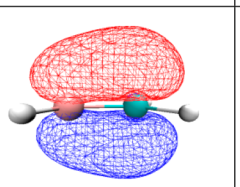	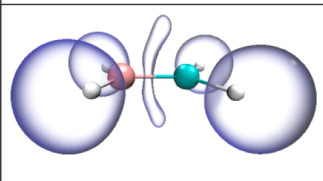	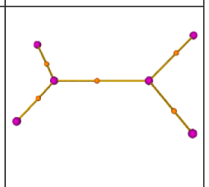
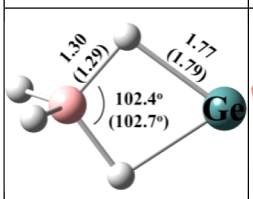	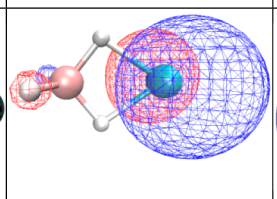	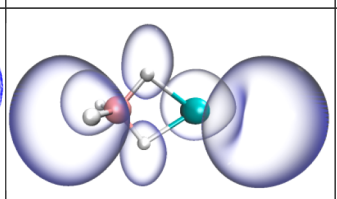	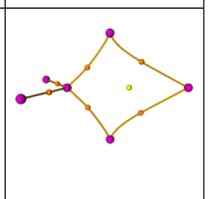
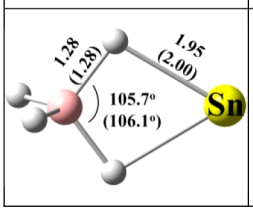	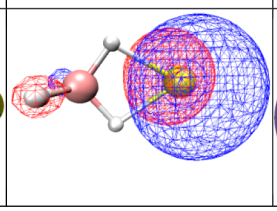	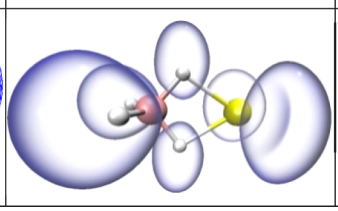	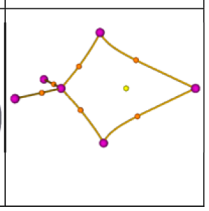

[a]Structural parameters calculated at the B3LYP/def2-TZVPP level are also given in parentheses (units in ångstrom and deg).

DOI: 10.1021/acs.inorgchem.7b03109
Inorg. Chem. XXXX, XXX, XXX−XXX

bond and the formation of Ge(μ-H)$_2$BH$_2$, which is only 1.1 kcal/mol lower in energy than H_2GeBH_2. However, only Sn(μ-H)$_2$BH$_2$ was identified in the reaction of boron atoms with SnH_4 from our experiment. The CCSD(t) calculations indicate that the Sn(μ-H)$_2$BH$_2$ molecule is 23.6 kcal/mol lower in energy than H_2BSnH_2 molecule. The isomerization from H_2SnBH_2 to Sn(μ-H)$_2$BH$_2$ take place in a two-step process by the rearrangement of two hydrogen atoms with corresponding barriers of 15.4 and 9.8 kcal/mol (Figure 7). Both steps are thermodynamically favored, and the energy needed to surmount the reaction barrier can be supplied by the internal energy of hot [H_2BSnH_2]* molecules produced by the reaction of B + SnH_4 before being quenched by the matrix.

It is well-known that for the structure of heavier main group ethylene analogues (e.g., H_2GeGeH_2 H_2SiSiH_2, H_2SiGeH_2) a trans-pyramidalized configuration is favored against the planar ethylene structure due to pseudo-Jahn−Teller mixing of the π bonding and σ* levels.[41−43] This molecular orbital mixing takes place more readily in the heavier main group element derivatives. However, for our H_2GeBH_2 molecule quantum-chemical calculations at the B3LYP and CCSD(T) levels predict a planar structure with $^2B_1$ ground state. This planar structure is also expected based on the Goddard−Malrieu−Trinquier model,[44] as the singlet−triplet gap of GeH_2 (18.5 kcal/mol) is much less than half of the interaction energy (96.8 kcal/mol) of BH_2 and GeH_2. Similar structure was predicted for H_2BSiH_2 that was trapped in low temperature matrix;[19] however, the H_2SnBH_2 molecule was not isolated in our experiment although the planar structure is predicted from our theoretical calculations.

A topological analysis of the electron density of H_2GeBH_2, Ge(μ-H)$_2$BH$_2$, and Sn(μ-H)$_2$BH$_2$ have been carried out at the B3LYP level of theory to gain more insight into the nature of these interactions. The bond critical point in the B−Ge interaction region of H_2GeBH_2 possesses negative values of energy density (−0.074) and the Laplacian (−0.170) at the bond critical point in the AIM analysis (see Table 5), which is typical for a covalent bond.[35] An ELF analysis[34] revealed that the disynaptic basin V(B,Ge) between the boron and germanium atoms is occupied by 2.93 e. This indicates the formation of a three electron multiple bond between boron and germanium. Further NBO analysis suggests σ-bond formation by the interaction of a sp^2 hybrid orbital of boron with a sp^2 hybrid orbital of germanium. The singly occupied orbital of π character is perpendicular to the molecular plane (Table 5) and built by the Ge $4p_z$ orbital and an empty $2p_z$ orbital of boron. The orbital overlap results in a donation of 0.32 e from $4p_z$-AO of germanium to the empty $2p_z$-AO of boron in H_2GeBH_2, which stabilizes the molecule even more, due to the unfavored empty $2p$-orbital of boron.[45]

Beyond this structural motif heavier group 14 element hydrides show also the tendency to form hydrogen bridged bonds. Tetrahydroborate complexes E(μ-H)$_2$BH$_2$ were observed in argon matrix for E = Si, Ge and Sn, while no bridged structure were found for BCH_4 in argon matrices, which is not stable predicted by quantum chemical calculations. The $[BH_4]^-$ forms covalent complexes with several transition metals, lanthanides and actinides, in which the B−H_t stretches usually appear in the region of 2400−2600 cm^{-1}.[38] An ionic character of these species tends to lower the B−H_t stretching vibrations (e.g., the B−H_t stretching of $NaBH_4$[46] appeared at 2274 cm^{-1}). From the AIM analysis, four bond critical point linking the bridged H atoms with B and E (E = Ge and Sn) by bond path and a ring critical point enclosed by the two hydrogen bridges have been found (Table 5). The bond critical points between Ge/Sn and bridged H atoms possess positive value of Laplacian value 0.099/0.118 and negative value of electron energy density −0.026/-0.012, which is common for a dative covalent bond.[47] In the picture of ELF, two trisynaptic basins occupied by about two electrons between B, H and E (E = Ge and Sn) corresponding to two 3c-2e hydrogen bridged bonds were identified. Consistent with both, the AIM and ELF analysis also the NBO analysis indicates a dative bond, where the B−H σ bonds donate electrons into the empty $4p$ orbitals of the Ge atom. The computed MP2 energy for this interaction accounts to E_2 = 73.2 kcal/mol in Ge(μ-H)$_2$BH$_2$ and to 47.6 kcal/mol in Sn(μ-H)$_2$BH$_2$, while the back-donation into the B−H σ* orbital is almost negligible.[48] In conclusion, dual 3c-2e bonds were formed in both Ge(μ-H)$_2$BH$_2$ and Sn(μ-H)$_2$BH$_2$ complexes through two hydrogen bridged bonds.

■ CONCLUSION

Our investigation clearly shows that ground state boron atoms insert spontaneously into the Ge−H bonds of germane to form H_2GeBH_2 on annealing in solid argon. This molecule further isomerize under λ = 405 nm irradiation to the slightly more stable Ge(μ-H)$_2$BH$_2$ isomer. In the reaction of boron with SnH_4 only Sn(μ-H)$_2$BH$_2$ molecule was produced. The electronic structure analysis for E(μ-H)$_2$BH$_2$ (E = Ge and Sn) support two 3c−2e hydrogen bridged E−H−B bonds. H_2GeBH_2 possesses a planar structure with an electron deficient B−Ge bond with a partial multiple bond character (bond order = 1.5). The bond orbital analysis indicates a polarized (32% B + 68% Ge) singly occupied π orbital. Furthermore, a substantial spin density on B at the expense of Ge substantiates this π bonding interaction. Thus, a new class of electron deficient germylidene complex is reported.

■ ASSOCIATED CONTENT

Supporting Information

The Supporting Information is available free of charge on the ACS Publications website at DOI: 10.1021/acs.inorgchem.7b03109.

Calculated vibrational frequencies and predicted intensities and atomic coordinates (PDF)

■ AUTHOR INFORMATION

Corresponding Authors

*E-mail: xfwang@tongji.edu.cn.
*E-mail: s.riedel@fu-berlin.de.

ORCID

Xuefeng Wang: 0000-0001-6588-997X
Sebastian Riedel: 0000-0003-4552-5719

Notes

The authors declare no competing financial interest.

■ ACKNOWLEDGMENTS

This work is supported by the National Natural Science Foundation of China (No. 21373152) and the International Exchange Program for Graduate Students, Tongji University (No. 2015020029). We thank X. Q. Zeng for GeH_4 and GeD_4 sample preparation.

DOI: 10.1021/acs.inorgchem.7b03109
Inorg. Chem. XXXX, XXX, XXX−XXX

REFERENCES

(1) Chatgilialoglu, C. Structural and Chemical Properties of Silyl Radicals. *Chem. Rev.* **1995**, *95* (5), 1229−1251.

(2) Chatgilialoglu, C. Organosilanes as radical-based reducing agents in synthesis. *Acc. Chem. Res.* **1992**, *25* (4), 188−194.

(3) Carland, M. W.; Schiesser, C. H. *Synthetic Uses of R_3MH (M = Ge, Sn, Pb), in Patai's Chemistry of Functional Groups*; John Wiley & Sons, Ltd., 2009.

(4) Chatgilialoglu, C.; Newcomb, M. Hydrogen Donor Abilities of the Group 14 Hydrides. *Adv. Organomet. Chem.* **1999**, *44*, 67−112.

(5) Eichler, B. E.; Power, P. P. $[2,6\text{-Trip}_2H_3C_6Sn(\mu\text{-H})]_2$ (Trip = C_6H_2-2,4,6-i-Pr_3): Synthesis and Structure of a Divalent Group 14 Element Hydride. *J. Am. Chem. Soc.* **2000**, *122* (36), 8785−8786.

(6) Thimer, K. C.; Al-Rafia, S. M. I.; Ferguson, M. J.; McDonald, R.; Rivard, E. Donor/acceptor stabilization of Ge(II) dihydride. *Chem. Commun.* **2009**, *46*, 7119−7121.

(7) Al-Rafia, S. M. I.; Malcolm, A. C.; Liew, S. K.; Ferguson, M. J.; Rivard, E. Stabilization of the Heavy Methylene Analogues, GeH2 and SnH2, within the Coordination Sphere of a Transition Metal. *J. Am. Chem. Soc.* **2011**, *133* (4), 777−779.

(8) Swarnakar, A. K.; McDonald, S. M.; Deutsch, K. C.; Choi, P.; Ferguson, M. J.; McDonald, R.; Rivard, E. Application of the Donor−Acceptor Concept to Intercept Low Oxidation State Group 14 Element Hydrides using a Wittig Reagent as a Lewis Base. *Inorg. Chem.* **2014**, *53* (16), 8662−8671.

(9) Rivard, E. Group 14 inorganic hydrocarbon analogues. *Chem. Soc. Rev.* **2016**, *45* (4), 989−1003.

(10) Power, P. P. Interaction of Multiple Bonded and Unsaturated Heavier Main Group Compounds with Hydrogen, Ammonia, Olefins, and Related Molecules. *Acc. Chem. Res.* **2011**, *44* (8), 627−637.

(11) Power, P. P. Main-group elements as transition metals. *Nature* **2010**, *463* (7278), 171−177.

(12) Spikes, G. H.; Fettinger, J. C.; Power, P. P. Facile Activation of Dihydrogen by an Unsaturated Heavier Main Group Compound. *J. Am. Chem. Soc.* **2005**, *127* (35), 12232−12233.

(13) Peng, Y.; Ellis, B. D.; Wang, X.; Fettinger, J. C.; Power, P. P. Reversible reactions of ethylene with distannynes under ambient conditions. *Science* **2009**, *325* (5948), 1668.

(14) Mandal, S. K.; Roesky, H. W. Group 14 Hydrides with Low Valent Elements for Activation of Small Molecules. *Acc. Chem. Res.* **2012**, *45* (2), 298−307.

(15) Guo, J.-D.; Liptrot, D. J.; Nagase, S.; Power, P. P. The multiple bonding in heavier group 14 element alkene analogues is stabilized mainly by dispersion force effects. *Chemical Science* **2015**, *6* (11), 6235−6244.

(16) Fischer, R. C.; Power, P. P. π-Bonding and the Lone Pair Effect in Multiple Bonds Involving Heavier Main Group Elements: Developments in the New Millennium. *Chem. Rev.* **2010**, *110* (7), 3877−3923.

(17) Al-Rafia, S. M. I.; Momeni, M. R.; Ferguson, M. J.; McDonald, R.; Brown, A.; Rivard, E. Stable Complexes of Parent Digermene: An Inorganic Analogue of Ethylene. *Organometallics* **2013**, *32* (22), 6658−6665.

(18) Al-Rafia, S. M. I.; Malcolm, A. C.; McDonald, R.; Ferguson, M. J.; Rivard, E. Trapping the Parent Inorganic Ethylenes H_2SiGeH_2 and H_2SiSnH_2 in the Form of Stable Adducts at Ambient Temperature. *Angew. Chem., Int. Ed.* **2011**, *50* (36), 8354−8357.

(19) Zhao, J.; Xu, B.; Yu, W. J.; Wang, X. F. Silicon Tetrahydroborate and Silylene Dihydroborate with Interelement B-H-Si and B = Si Bonds. *Organometallics* **2016**, *35* (19), 3272−3280.

(20) Di Pietro, E.; Cardini, G.; Schettino, V. Ab initio molecular dynamics study of the hydrolysis reaction of diborane. *Phys. Chem. Chem. Phys.* **2007**, *9* (29), 3857−3863.

(21) Porter, R. F.; Gupta, S. K. Heats of Formation of Gaseous H_2BOH and $HB(OH)_2$. *J. Phys. Chem.* **1964**, *68* (9), 2732−2733.

(22) Bernardi, F.; Bottoni, A.; Epiotis, N. D. Quantitative nonempirical analysis of the.pi.-conjugative effects of substituents. *J. Am. Chem. Soc.* **1978**, *100* (23), 7205−7209.

(23) Magnusson, E. Substituent effects in second row molecules. *Tetrahedron* **1985**, *41* (14), 2939−2943.

(24) Carpenter, J. D.; Ault, B. S. Matrix isolation study of the reaction of diborane with hydrogen sulfide: spectroscopic characterization of mercaptoborane, H_2BSH. *J. Phys. Chem.* **1992**, *96* (20), 7913−7916.

(25) Carpenter, J. D.; Ault, B. S. Matrix isolation study of the reactions of diborane with pyridine, pyrrole, and pyrrolidine: spectroscopic characterization of $C_4H_9N{\cdot}BH_3$ and pyrrolidinoborane. *J. Phys. Chem.* **1993**, *97* (44), 11397−11401.

(26) Withnall, R.; Andrews, L. Matrix reactions of germane and oxygen atoms: infrared spectroscopic evidence of germylene-water complex, germanone, germanol, hydroxygermylene, and germanic acid. *J. Phys. Chem.* **1990**, *94* (6), 2351−2357.

(27) Becke, A. D. Density - functional thermochemistry. III. The role of exact exchange. *J. Chem. Phys.* **1993**, *98* (7), 5648−5652.

(28) Lee, C.; Yang, W.; Parr, R. G. Development of the Colle-Salvetti correlation-energy formula into a functional of the electron density. *Phys. Rev. B: Condens. Matter Mater. Phys.* **1988**, *37* (2), 785.

(29) Weigend, F.; Ahlrichs, R. Balanced basis sets of split valence, triple zeta valence and quadruple zeta valence quality for H to Rn: Design and assessment of accuracy. *Phys. Chem. Chem. Phys.* **2005**, *7* (18), 3297−3305.

(30) Metz, B.; Stoll, H.; Dolg, M. Small-core multiconfiguration-Dirac−Hartree−Fock-adjusted pseudopotentials for post-d main group elements: Application to PbH and PbO. *J. Chem. Phys.* **2000**, *113* (7), 2563−2569.

(31) Frisch, M. J.; Trucks, G. W.; Schlegel, H. B.; Scuseria, G. E.; Robb, M. A.; Cheeseman, J. R.; Scalmani, G.; Barone, V.; Mennucci, B.; Petersson, G. A.; Nakatsuji, H.; Caricato, M.; Li, X.; Hratchian, H. P.; Izmaylov, A. F.; Bloino, J.; Zheng, G.; Sonnenberg, J. L.; Hada, M.; Ehara, M.; Toyota, K.; Fukuda, R.; Hasegawa, J.; Ishida, M.; Nakajima, T.; Honda, Y.; Kitao, O.; Nakai, H.; Vreven, T.; Montgomery, J. A., Jr.; Peralta, J. E.; Ogliaro, F.; Bearpark, M.; Heyd, J. J.; Brothers, E.; Kudin, K. N.; Staroverov, V. N.; Kobayashi, R.; Normand, J.; Raghavachari, K.; Rendell, A.; Burant, J. C.; Iyengar, S. S.; Tomasi, J.; Cossi, M.; Rega, N.; Millam, N. J.; Klene, M.; Knox, J. E.; Cross, J. B.; Bakken, V.; Adamo, C.; Jaramillo, J.; Gomperts, R.; Stratmann, R. E.; Yazyev, O.; Austin, A. J.; Cammi, R.; Pomelli, C.; Ochterski, J. W.; Martin, R. L.; Morokuma, K.; Zakrzewski, V. G.; Voth, G. A.; Salvador, P.; Dannenberg, J. J.; Dapprich, S.; Daniels, A. D.; Farkas, Ö.; Foresman, J. B.; Ortiz, J. V.; Cioslowski, J.; Fox, D. J. *Gaussian 09*, revision A.01; Gaussian, Inc.: Wallingford, CT, 2009.

(32) CFOUR, Coupled-Cluster techniques for Computational Chemistry, a quantum-chemical program package by Stanton, J. F.; Gauss, J.; Harding, M. E.; Szalay, P. G. with contributions from Auer, A. A.; Bartlett, R. J.; Benedikt, U.; Berger, C.; Bernholdt, D. E.; Bomble, Y. J.; Cheng, L.; Christiansen, O.; Heckert, M.; Heun, O.; Huber, C.; Jagau, T.-C.; Jonsson, D.; Jusélius, J., Klein, K.; Lauderdale, W. J.; Matthews, D. A.; Metzroth, T.; Mück, L. A., O'Neill, D. P., Price, D. R.; Prochnow, E.; Puzzarini, C.; Ruud, K.; Schiffmann, F.; Schwalbach, W.; Simmons, C.; Stopkowicz, S.; Tajti, A.; Vázquez, J., Wang, F.; Watts, J. D. and the integral packages MOLECULE (Almlöf, J.; Taylor, P. R.), PROPS (Taylor, P. R.), ABACUS (Helgaker, T.; Jensen, H. J. Aa.; Jørgensen, P.; Olsen, J.), and ECP routines by Mitin, A. V.; van Wüllen, C.. For the current version, see http://www.cfour.de.

(33) Lu, T.; Chen, F. Multiwfn: A multifunctional wavefunction analyzer. *J. Comput. Chem.* **2012**, *33* (5), 580.

(34) Savin, A.; Nesper, R.; Wengert, S.; Fässler, T. F. ELF: The electron localization function. *Angew. Chem., Int. Ed. Engl.* **1997**, *36* (17), 1808−1832.

(35) Bader, R. F. W. Atoms in molecules. *Acc. Chem. Res.* **1985**, *18* (1), 9−15.

(36) Wang, X. F.; Andrews, L.; Kushto, G. P. Infrared Spectra of the Novel Ge_2H_2 and Ge_2H_4 Species and the Reactive $GeH_{1,2,3}$ Intermediates in Solid Neon, Deuterium and Argon. *J. Phys. Chem. A* **2002**, *106* (24), 5809−5816.

(37) Marks, T. J.; Kennelly, W. J.; Kolb, J. R.; Shimp, L. A. Structure and dynamics in metal tetrahydroborates. II. Vibrational spectra and

DOI: 10.1021/acs.inorgchem.7b03109
Inorg. Chem. XXXX, XXX, XXX−XXX

structures of some transition metal and actinide tetrahydroborates. *Inorg. Chem.* **1972**, *11* (10), 2540−2546.
(38) Marks, T. J.; Kolb, J. R. Covalent transition metal, lanthanide, and actinide tetrahydroborate complexes. *Chem. Rev.* **1977**, *77* (2), 263−293.
(39) Hassanzadeh, P.; Hannachi, Y.; Andrews, L. Pulsed laser evaporated boron atom reactions with methane. 2. Infrared spectra of H_2CBH_2, H_2CBH, HCBH, and HBCBH in solid argon. *J. Phys. Chem.* **1993**, *97* (24), 6418−6424.
(40) Schmidt, M. W.; Baldridge, K. K.; Boatz, J. A.; Elbert, S. T.; Gordon, M. S.; Jensen, J. H.; Koseki, S.; Matsunaga, N.; Nguyen, K. A.; Su, S.; Windus, T. L.; Dupuis, M.; Montgomery, J. A. General atomic and molecular electronic structure system. *J. Comput. Chem.* **1993**, *14* (11), 1347−1363.
(41) Trinquier, G. Double bonds and bridged structures in the heavier analogues of ethylene. *J. Am. Chem. Soc.* **1990**, *112*, 2130−2131.
(42) Grev, R. S. Structure and Bonding in the Parent Hydrides and Multiply Bonded Silicon and Germanium Compounds: From MH_n to $R_2M = M'R_2$ and $RM \equiv M'R$. *Adv. Organomet. Chem.* **1991**, *33*, 125−170.
(43) Pearson, R. G. Concerning Jahn-Teller Effects. *Proc. Natl. Acad. Sci. U. S. A.* **1975**, *72* (6), 2104−2106.
(44) Driess, M.; Grützmacher, H. Main Group Element Analogues of Carbenes, Olefins, and Small Rings. *Angew. Chem., Int. Ed. Engl.* **1996**, *35* (8), 828−856.
(45) Osorio, E.; Olson, J. K.; Tiznado, W.; Boldyrev, A. I. Analysis of Why Boron Avoids sp2 Hybridization and Classical Structures in the B_nH_{n+2} Series. *Chem. - Eur. J.* **2012**, *18* (31), 9677−9681.
(46) Price, W. C. The Infrared Absorption Spectra of Some Metal Borohydrides. *J. Chem. Phys.* **1949**, *17* (11), 1044−1052.
(47) Cremer, D.; Kraka, E. A Description of the Chemical Bond in Terms of Local Properties of Electron Density and Energy. *Croat. Chem. Acta* **1984**, *57* (6), 1259−1281.
(48) Reed, A. E.; et al. Intermolecular interactions from a natural bond orbital, donor-acceptor viewpoint. *Chem. Rev.* **1988**, *88* (6), 899−926.

DOI: 10.1021/acs.inorgchem.7b03109
Inorg. Chem. XXXX, XXX, XXX−XXX